

Reconfigurable Optical Inter-Channel Interference Mitigation for Spectrally Overlapped QPSK Signals using Nonlinear Wave Mixing in Cascaded PPLN Waveguides

YINWEN CAO,^{1,*} MORTEZA ZIYADI,¹ AMIRHOSSEIN MOHAJERIN-ARIAEI,¹
AHMED ALMAIMAN,¹ PEICHENG LIAO,¹ CHANGJING BAO,¹ FATEMEH ALISHAHI,¹
AHMAD FALAHPOUR,¹ BISHARA SHAMEE,¹ JENG-YUAN YANG,² YOUICHI AKASAKA,²
MOTOYOSHI SEKIYA,² MOSHE TUR,³ CARSTEN LANGROCK,⁴ MARTIN FEJER,⁴
JOSEPH TOUCH,⁵ AND ALAN E. WILLNER¹

¹ Department of Electrical Engineering, University of Southern California, Los Angeles, CA 90089, USA

² Fujitsu Laboratories of America, 2801 Telecom Parkway, Richardson, TX 75082, USA

³ School of Electrical Engineering, Tel Aviv University, Ramat Aviv 69978, Israel

⁴ Edward L. Ginzton Laboratory, 348 Via Pueblo Mall, Stanford University, Stanford, CA 94305, USA

⁵ Information Sciences Institute, University of Southern California, Marina del Rey, CA 90292, USA

*Corresponding author: yinwenca@usc.edu

Received XX Month XXXX; revised XX Month, XXXX; accepted XX Month XXXX; posted XX Month XXXX (Doc. ID XXXXX); published XX Month XXXX

A reconfigurable all optical inter-channel interference (ICI) mitigation method is proposed for an overlapped channel system that avoids the need for multiple-channel detection and channel spacing estimation. The system exhibits 0.5dB implementation penalty compared with a single channel baseline system. Experiments using a dual-carrier QPSK overlapped system with both 20G-baud and 25G-baud under different channel spacing conditions evaluate the performance of the method. Improved signal constellation and receiver sensitivity demonstrate the effectiveness of this approach. This results in over 4dB OSNR benefit when the system Q factor reaches forward error correction (FEC) threshold of 8.5dB under less-than-baudrate channel spacing conditions.

OCIS codes: (060.2360) Fiber optics links and subsystems; (060.4370) Nonlinear optics, fibers.

<http://dx.doi.org/10.1364/OL.99.099999>

The use of digital signal processing (DSP) in coherent receivers is a major advance in optical communications of recent years [1-4]. One capability of DSP is to mitigate inter-channel interference (ICI), which is a typical crosstalk phenomenon arising from the

allocation of different channels with channel spacing near to the baud rate for high spectral efficiency [5-7]. A common approach to mitigate ICI in the resultant spectrally overlapped channels is to use a digital multi-channel equalization based on different algorithms after photodetection, which usually requires receiving all the relevant channels that contribute to the ICI for the channel of interest [8-17]. This approach can be achieved using either one receiver with a large electrical bandwidth [9] or several synchronized typical receivers with limited bandwidth, each responsible for acquiring a different channel [10-13].

One motivation for exploring an optical-domain approach is to mitigate ICI before detection, so that only one typical receiver is needed for the target channel. Other motivations for implementing optical ICI mitigation might include: i) the potential for high-speed signal processing [18]; ii) avoiding accurate channel spacing estimation (10MHz estimation error could significantly degrade the performance of digital multi-channel equalization) [8]; iii) freedom from optoelectronic conversion, which might be preferable for signal regeneration in the middle of the link.

There have been several works which attempt to use optical signal processing to mitigate inter-symbol interference (ISI) caused by fiber link distortion such as chromatic dispersion [19, 20]. However, to the best of our knowledge, optical signal processing has not been used to mitigate the ICI effect in spectrally overlapped channels.

In this paper, an optical ICI mitigation scheme based on the nonlinear wave mixing in periodically poled lithium niobate (PPLN) waveguides is proposed. The implementation penalty of this scheme is about 0.5dB compared with a single channel back-to-back (B2B) baseline configuration. The performance of the proposed method is evaluated experimentally by a dual-carrier QPSK overlapped system with both 20G-baud and 25G-baud [21] under four different channel spacing conditions.

Figure 1 describes the proposed optical ICI mitigation scheme as composed of three stages. At the input, two channels S_1 and S_2 are partially overlapped with a certain channel spacing Δf . The entire signal is expressed as follows:

$$S = S_1(f - \Delta f/2) + S_2(f + \Delta f/2). \quad (1)$$

In the first stage of Fig. 1, a conjugate copy is generated by sending S and a pump P through a PPLN waveguide via the cascaded processes of second-harmonic-generation (SHG) and difference-harmonic-generation (DFG). The conjugate copy is also partially overlapped, which is denoted as:

$$S^* = S_1^*(2f_p - f + \Delta f/2) + S_2^*(2f_p - f - \Delta f/2), \quad (2)$$

in which f_p denotes the frequency of the pump P . In the second stage, an optical programmable filter is utilized to select desired channels (S'_1, S'_2) or (S'_2, S'_1) and modify the amplitudes and phases of S_1^* or S_2^* by multiplying a complex coefficient (c_1 or c_2) as in Fig. 1. Here

$$S'_1 \approx S_1(f - \Delta f/2) + \gamma_1 S_2(f + \Delta f/2), \quad (3)$$

$$S'_2 \approx S_2(f + \Delta f/2) + \gamma_2 S_1(f - \Delta f/2), \quad (4)$$

$$S_1^* \approx S_1^*(2f_p - f + \Delta f/2) + \gamma_3 S_2^*(2f_p - f - \Delta f/2), \quad (5)$$

$$S_2^* \approx S_2^*(2f_p - f - \Delta f/2) + \gamma_4 S_1^*(2f_p - f + \Delta f/2). \quad (6)$$

The above equations are similar to [13, 22] in which the second terms are ICI crosstalk and $\gamma_i < 1$ ($i = 1, 2, 3, 4$) depends on the frequency characteristics of the optical programmable filter. Due to channel overlap, the spectra envelopes of the four selected channels at the second stage in Fig. 1 are asymmetric. For ICI mitigation of S_1 , at Port 1, S'_1 and S_2^* are selected while S_2^* is multiplied by c_2 , whose value is determined by the current ICI impact. Pump P is also retained in this stage to maintain coherence in the next stage process. In the third stage, through SHG and DFG in another PPLN waveguide, $c_2 S_2^*$ is added back to S'_1 as

$$\hat{S}_1 = (1 + c_2^* \gamma_4^*) S_1(f - \Delta f/2) + (\gamma_1 + c_2^*) S_2(f + \Delta f/2). \quad (7)$$

By tuning c_2 , the crosstalk term can be reduced. However, the ICI crosstalk cannot be fully compensated because γ_i is not a constant in the frequency domain. Since the pump P is preserved, $c_2^* S_2^*$ is added to S'_1 with the exact channel spacing of Δf , which is why accurate estimation of Δf is unnecessary. The processed channel is then filtered as $\hat{S}'_1 = H_f \hat{S}_1$ with residual ICI and sent to the detector (H_f represents the filter transfer function). For ICI mitigation of S_2 , a similar set of operations are carried out at Port 2, in which the pump P , S'_2 and $c_1 S_1^*$ are selected.

Figure 2(a) illustrates the experimental setup of optical ICI mitigation of a QPSK modulation format in a two-overlapped-channel system. Two separate source lasers are modulated by independent QPSK modulators with uncorrelated data streams. A polarization controller (PC) is added after the QPSK Modulator-1 in Fig. 2 to ensure that the two channels have the same polarization which maximizes the ICI effect. Pre-amplifiers are placed in the link of both channels to maintain the same signal power for the channels which are then combined by a 50/50 coupler to produce the overlapped channels.

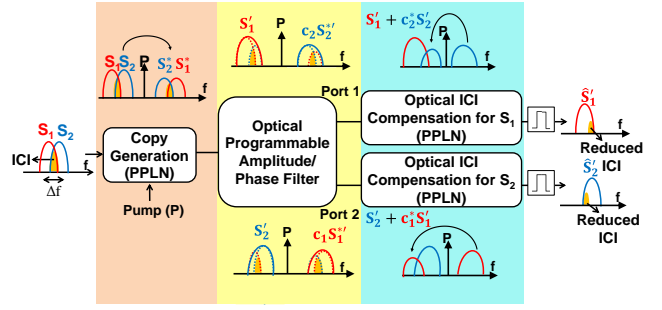


Fig. 1. Conceptual diagram of the proposed optical ICI mitigation scheme for an overlapped channel system. There are three processing stages in the background with different colors: 1) channel copy generation; 2) complex coefficients adjustment; 3) channel addition. PPLN: periodically poled lithium niobate.

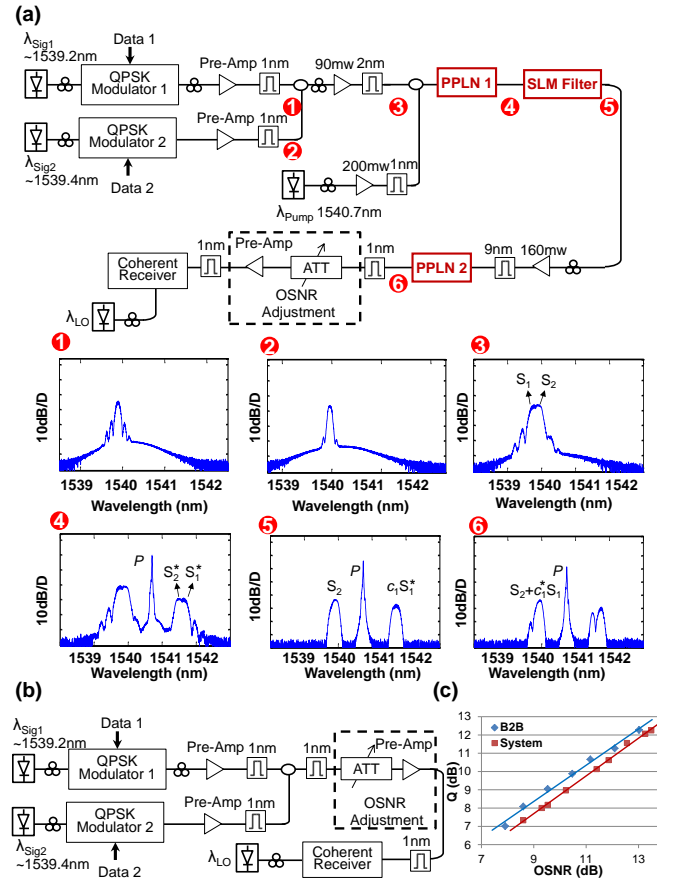


Fig. 2. (a) Experimental setup for the ICI mitigation system and the corresponding optical spectra: 1) Channel-1 before overlapping, 2) Channel-2 before overlapping, 3) overlapped channels, 4) copy generation, 5) filtering and coefficient adjustment, 6) channel addition. (b) Back-to-back (B2B) baseline configuration. (c) System implementation penalty compared with B2B baseline configuration under single channel transmission.

For optical ICI mitigation, the overlapped channels are amplified to 90mW and sent into the first PPLN waveguide along with 200mW pump at the wavelength of 1540.7nm. The quasi-phase matching (QPM) wavelength is temperature-tuned and stabilized at around 1541nm to produce the highest conversion efficiency. After that, the conjugated copies of the channels are generated and

the spectra are shown in the insets of Fig. 2(a). Because the channels are partially overlapped, only about half of each channel spectrum is visible. In the next stage, all the components are sent through a spatial light modulator (SLM) filter, based on liquid crystal on silicon (LCoS) technology, for channel selection and amplitude/phase adjustment. For ICI mitigation of S_2 , the outputs of the SLM filter are S'_2 , $c_1 S'_1$ and P , whose spectra are shown in Fig. 2(a). These three components are injected into the second PPLN waveguide, where $c_1 S'_1$ is added back onto S_2 as $S_2 + c_1 S'_1$ with the precise channel spacing of Δf . Finally, a filter and OSNR adjustment are added before the coherent receiver in which signal quality is evaluated and bit errors are counted. For OSNR adjustment, the output power of the pre-amplifier prior to the coherent receiver is fixed. By attenuating the signal, different levels of amplified spontaneous emission (ASE) are loaded to vary the OSNR. Similar operations are implemented on the S_1 channel to generate $S'_1 + c_2 S'_2$ for the ICI mitigation. Figure 2(b) is the back-to-back (B2B) baseline counterpart, in which the overlapped channels are generated at the transmitter in the same manner while the 1nm filter and electrical filter in the same coherent receiver are both centered on the target channel carrier for signal selection as in Fig. 2(a). The implementation penalty of the proposed ICI mitigation system is measured by comparing with a single channel B2B baseline configuration. In this scenario, there is only a single channel without ICI crosstalk. Because nonlinear noise is primarily generated during the nonlinear wave mixing stages, the signal quality is expected to degrade. Figure 2(c) shows that, for the same system Q factor, 0.5dB OSNR penalty is observed in the proposed optical ICI mitigation system.

The performance of the proposed ICI mitigation method is first assessed using a dual-carrier 20G-baud QPSK signal with channel spacing (CS) of 15GHz, 17.5GHz, 20GHz, and 25GHz. The signal constellation comparisons are shown in Fig. 3(a). To emphasize the ICI effect, there is no spectrum shaping or filtering at the transmitter. When CS is 25GHz, which is much larger than the baudrate of the signal, the ICI effect is insignificant and the proposed ICI mitigation method provides negligible benefit. The difference between the signal constellations of the two channels might attribute to the fact that the two channels are generated by separate modulators, which would produce different signal quality. When CS is equal to or less than the baudrate, the effect of ICI becomes significant. In the meantime, the improvement due to ICI mitigation turns to be noticeable. However, the ICI effect cannot be completely compensated [9], so even after ICI mitigation, the signal quality with a smaller CS is still worse than the signal quality with a larger CS, as shown in Fig. 3(a). To demonstrate the tunability of the proposed scheme, the baudrate of both QPSK channels is changed to 25G-baud and four different CS (20GHz, 22.5GHz, 25GHz and 30GHz) are selected accordingly. These additional constellation comparisons are depicted in Fig. 3(b). As was observed earlier, when CS is 30GHz, which is much larger than the signal baudrate, the ICI effect is insignificant and the benefit of ICI mitigation is negligible. However, when CS decreases to or below the baudrate, the effect of ICI becomes increasingly significant and the improvement from ICI mitigation grows accordingly. Still, the signal quality with smaller CS remains worse than the signal quality with larger CS as shown in Fig. 3(b).

As a further evaluation, the Q factors under different CS conditions are calculated and compared. Figure 4 shows Q factor curves for both 20G-baud and 25G-baud systems under different

CS conditions. The cross and square symbols represent Q factors for 20G-baud and 25G-baud systems with ICI mitigation. The triangle and diamond symbols denote Q factors for 20G-baud and 25G-baud systems with B2B baseline configurations. In Fig. 4(a), CS is 5GHz smaller than the baudrate and the Q factor is below the FEC threshold of 8.5dB without ICI mitigation. Meanwhile, the proposed ICI mitigation makes the system Q factor exceed the FEC threshold. When CS increases but remains no larger than the baudrate, the ICI mitigation brings significant benefit, as shown in Figs. 4(b) and 4(c). An OSNR benefit of more than 4dB is observed when the system Q factor reaches the FEC threshold. When CS is much larger than the baudrate as in Fig. 4(d), the Q factor curves almost overlap, indicating that the proposed ICI mitigation method brings little improvement since the ICI effect is already very small. Because the coefficient c_i ($i=1, 2$) is complex, not only the amplitude but also the phase will affect the system performance.

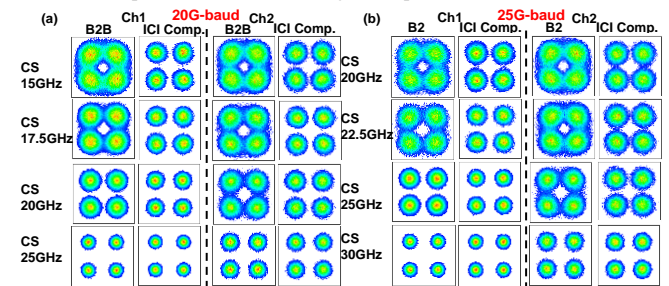


Fig. 3. Signal constellations comparison with and without ICI mitigation for (a) 20G-baud and (b) 25G-baud overlapped channel systems of different channel spacing (CS).

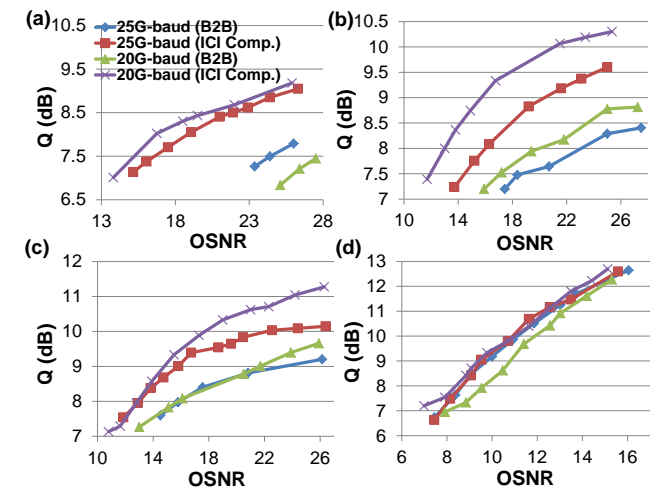


Fig. 4. Q factor comparison with and without ICI mitigation under different channel spacing (CS) and baud rates. (a) 25G-baud with 20GHz CS and 20G-baud with 15GHz CS; (b) 25G-baud with 22.5GHz CS and 20G-baud with 17.5GHz CS; (c) 25G-baud with 25GHz CS and 20G-baud with 20GHz CS; (d) 25G-baud with 30GHz CS and 20G-baud with 25GHz CS.

Figure 5 shows the relationship between phase and system Q factor. The corresponding signal constellations are also depicted. It can be seen that there is an optimal phase which yields the highest Q factor.

Figure 6 illustrates VPI simulated EVM comparisons with and without the proposed ICI mitigation when an adaptive intra-channel equalizer with different tap numbers is employed

afterwards. The tap weights for the intra-channel equalizer are updated by constant modulus algorithm (CMA) [23]. As the tap number increases, both EVMs decrease and the signal quality with the proposed ICI mitigation is always better than the one without ICI mitigation. In the ICI mitigation stage, the optimal amplitude of the coefficient is approximately 0.45. When the overlapped spectrum is completely cut, the signal's EVM is increasing. The signal quality is degraded because part of the signal information has been erased. In the experiment, the original channels and the copies may experience different linear and nonlinear phase shift due to different wavelengths and power levels, and as a result, a non-zero relative phase is expected and the coefficient should be complex. However, for the simulation result in Fig. 6, the optimal phase for coefficient is zero because different phase shifts are not considered.

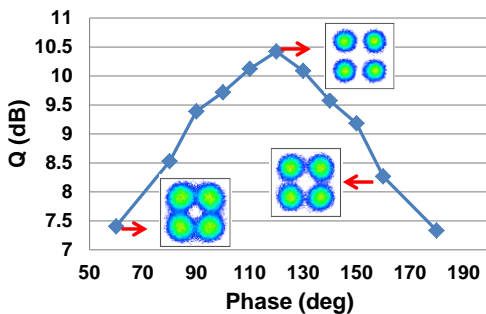


Fig. 5. System Q factor varies with the phase change of the coefficient and the corresponding signal constellation. Different phases can change the system Q factor by more than 3dB.

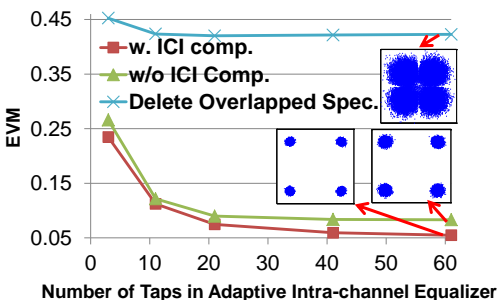


Fig. 6. Simulated EVM comparisons by employing an adaptive intra-channel equalizer with different tap numbers for three scenarios: 1) with proposed ICI mitigation; 2) without ICI mitigation; 3) cutting the overlapped spectrum.

In this paper, as a proof of concept, the coefficients for ICI mitigation are optimized manually by monitoring the signal EVM on the coherent receiver. For more practical applications, further research might be required to design a feedback loop for adaptive coefficient adjustment. It should also be noted that after long distance transmission, the cumulated dispersion would introduce delay between different channels. This effect needs to be compensated before implementing the proposed ICI migration scheme. In addition, because only one tap is currently employed in the proposed optical ICI mitigation scheme, performance might be worse compared with conventional DSP-based ICI mitigation approaches where more taps are available. However, when more copies can be generated in the PPLN waveguide with sufficient efficiency, more taps could be employed in the optical solution.

Together with the advantages such as free of multiple-channel detection and channel spacing estimation, a quantitative comparison between the proposed all optical mitigation scheme and conventional DSP-based methods might be interesting.

Although only two channels are considered in this paper, considering $\pm 10\text{nm}$ QPM bandwidth in PPLN waveguides, this approach could be extended to WDM channel system. In order to mitigate the ICI effect in N channels simultaneously, the output of the SLM filter would need to be divided into N ports with one PPLN waveguide in each path. The following power consumption and cost problems might be alleviated by an implementation of this approach as a photonics integrated circuit [24].

Funding. National Science Foundation (NSF); Center for Integrated Access Networks (CIAN); National Institute of Standards and Technology (NIST); Fujitsu Laboratories of America (FLA)

References

1. S. J. Savory, IEEE J. Sel. Top. Quantum Electron. **16**, 1164 (2010).
2. E. Ip, P. Ji, E. Mateo, Y.-K. Huang, L. Xu, D. Qian, N. Bai, and T. Wang, Proc. IEEE **100**, 1065 (2012).
3. D. Lavery, R. Maher, D. S. Millar, B. C. Thomsen, P. Bayvel and S. J. Savory, J. Lightwave Technol. **31**, 609 (2013).
4. K. Roberts, D. Beckett, D. Boertjes, J. Berthold and C. Laperle, IEEE Commun. Mag. **48**, 62 (2010).
5. J. Wang, C. Xie and Z. Pan, J. Lightwave Technol. **30**, 3679 (2012).
6. E. Connolly, A. Kaszubowska-Anandarajah and L. P. Barry, Photon. Technol. Lett., **19**, 616 (2007).
7. T. Koike-Akino, D. Millar, K. Kojima and K. Parsons, Proc. ECOC, Th.1.6.5 (2015).
8. J. Pan, A. Stark, C. Liu and S. E. Ralph, Proc. OFC, OW4B.6 (2013).
9. N. Kaneda, T. Pfau and J. Lee, Proc. ECOC, Th.2.C.1 (2013).
10. M. Sato, R. Maher, D. Lavery, K. Shi, B. C. Thomsen and P. Bayvel, J. Lightwave Technol. **33**, 1388 (2015).
11. C. Liu J. Pan, T. Detwiler, A. Stark, Y. T. Hsueh, G. K. Chang and S. E. Ralph, Proc. OFC, OTu21.4 (2013).
12. Tao Zeng, Opt. Express **21**, 14799 (2013).
13. F. Hamaoka, K. Saito, T. Matsuda and A. Naka, Proc. ECOC, Mo.3.5.5 (2014).
14. S. Chandrasekhar and Xiang Liu, Opt. Express **17**, 21350 (2009).
15. K. Shibahara, A. Masuda, S. Kawai and M. Fukutoku, Proc. ECOC, Th.1.6.4 (2015).
16. S. Yamamoto, K. Saito, A. Naka and H. Maeda, Proc. ECOC, Th.2.5.3 (2015).
17. F. Lehmann, P. Ramantanis and Y. Frignac, J. Opt. Commun. Netw. **6**, 315 (2014).
18. A. E. Willner, S. Khaleghi, M. Chitgarha, and O. Yilmaz, J. Lightwave Technol. **32**, 660 (2014).
19. P. J. Winzer, G. Raybon, C. R. Doerr, M. Duelk and C. Dorrer, J. Lightwave Technol. **24**, 3107 (2006).
20. S. Khaleghi, O. F. Yilmaz, M. R. Chitgarha, M. Tur, N. Ahmed, S. R. Nuccio, I. M. Fazal, X. Wu, M. W. Haney, C. Langrock, M. M. Fejer and A. E. Willner, Photon. J. **4**, 1220 (2012).
21. Y. Cao, M. Ziyadi, A. Mohajerin-Ariaei, A. Almairan, P. Liao, C. Bao, B. Shamee, J. Yang, Y. Akasaka, M. Sekiya, M. Tur, C. Langrock, M. Fejer, J. Touch and A. Willner, Proc. ECOC, P.3.17 (2015).
22. S. Yamamoto, K. Saito, F. Hamaoka, T. Matsuda, A. Naka and H. Maeda, J. Lightwave Technol. **34**, 2824 (2016).
23. J. Treichler and M. Larimore, IEEE Trans. Acoustics, Speech, and Signal Process. **33**, 420 (1985).
24. D. Moss, R. Morandotti, A. Gaeta, and M. Lipson, Nat. Photon. **7**, 597 (2013).

References (Long Format)

1. S. J. Savory, "Digital optical coherent receivers: Algorithms and subsystems," *IEEE J. Sel. Top. Quantum Electron.*, vol. 16, no. 5, pp. 1164–1179, 2010.
2. E. Ip, P. Ji, E. Mateo, Y.-K. Huang, L. Xu, D. Qian, N. Bai, and T. Wang, "100G and beyond transmission technologies for evolving optical networks and relevant physical-layer issues," *Proc. IEEE*, vol. 100, no. 5, pp. 1065–1078, May 2012.
3. D. Lavery, R. Maher, D. S. Millar, B. C. Thomsen, P. Bayvel and S. J. Savory, "Digital Coherent Receivers for Long-Reach Optical Access Networks," in *Journal of Lightwave Technology*, vol. 31, no. 4, pp. 609-620, Feb.15, 2013.
4. K. Roberts, D. Beckett, D. Boertjes, J. Berthold and C. Laperle, "100G and beyond with digital coherent signal processing," in *IEEE Communications Magazine*, vol. 48, no. 7, pp. 62-69, July 2010.
5. J. Wang, C. Xie and Z. Pan, "Generation of Spectrally Efficient Nyquist-WDM QPSK Signals Using Digital FIR or FDE Filters at Transmitters," in *Journal of Lightwave Technology*, vol. 30, no. 23, pp. 3679-3686, Dec.1, 2012.
6. E. Connolly, A. Kaszubowska-Anandarajah and L. P. Barry, "Cross Channel Interference due to Wavelength Drift of Tunable Lasers in DWDM Networks," in *IEEE Photonics Technology Letters*, vol. 19, no. 8, pp. 616-618, Apr. 15, 2007.
7. T. Koike-Akino, D. Millar, K. Kojima and K. Parsons, "Laser Frequency Drift Compensation with Han-Kobayashi Coding in Superchannel Nonlinear Optical Communications," *Optical Communication (ECOC)*, 40th European Conference and Exhibition on, paper Th.1.6.5, Valencia, 2015, pp. 1-3.
8. J. Pan, A. Stark, C. Liu and S. E. Ralph, "Fractionally-spaced frequency domain linear crosstalk cancellation with spectral alignment techniques for coherent superchannel optical systems," *Optical Fiber Communication Conference and Exposition and the National Fiber Optic Engineers Conference (OFC/NFOEC)*, paper OW4B.6, Anaheim, CA, 2013, pp. 1-3.
9. N. Kaneda, T. Pfau and J. Lee, "Frequency diversity MIMO detection for coherent optical transmission," *Optical Communication (ECOC)*, 39th European Conference and Exhibition on, paper Th.2.C.1, London, 2013, pp. 1-3.
10. M. Sato, R. Maher, D. Lavery, K. Shi, B. C. Thomsen and P. Bayvel, "Frequency Diversity MIMO Detection for DP- QAM Transmission," in *Journal of Lightwave Technology*, vol. 33, no. 7, pp. 1388-1394, 2015.
11. C. Liu J. Pan, T. Detwiler, A. Stark, Y. T. Hsueh, G. K. Chang and S. E. Ralph, "Joint ICI cancellation for superchannel coherent optical systems in nonlinear transmission regimes," *Optical Fiber Communication Conference and Exposition and the National Fiber Optic Engineers Conference (OFC/NFOEC)*, paper OTu21.4, Anaheim, CA, 2013, pp. 1-3.
12. Tao Zeng, "Superchannel transmission system based on multi-channel equalization," *Optics Express* 21, 14799-14807 (2013).
13. F. Hamaoka, K. Saito, T. Matsuda and A. Naka, "Super high density multi-carrier transmission system by MIMO processing," *Optical Communication (ECOC)*, 2014 European Conference on, paper Mo.3.5.5, Cannes, 2014, pp. 1-3.
14. S. Chandrasekhar and Xiang Liu, "Experimental investigation on the performance of closely spaced multi-carrier PDM-QPSK with digital coherent detection," *Optics Express* 17, 21350-21361 (2009).
15. K. Shibahara, A. Masuda, S. Kawai and M. Fukutoku, "Multi-stage successive interference cancellation for spectrally-efficient super-Nyquist transmission," *Optical Communication (ECOC)*, 2015 European Conference on, paper Th.1.6.4, Valencia, 2015, pp. 1-3.
16. S. Yamamoto, K. Saito, A. Naka and H. Maeda, "Compatibility between nonlinear compensation and crosstalk compensation using MIMO processing in super-high-density multi-carrier transmission system," *Optical Communication (ECOC)*, 2015 European Conference on, paper Th.2.5.3, Valencia, 2015, pp. 1-3.
17. F. Lehmann, P. Ramantanis and Y. Frignac, "Joint channel estimation, interference mitigation, and decoding for WDM coherent optical communications," in *IEEE/OSA Journal of Optical Communications and Networking*, vol. 6, no. 3, pp. 315-325, March 2014.
18. A. E. Willner, S. Khaleghi, M. Chitgarha, and O. Yilmaz, "All-Optical Signal Processing," *Invited Paper, IEEE/OSA Journal of Lightwave Technology*, vol. 32, no. 4, pp. 660-680, 2014.
19. P. J. Winzer, G. Raybon, C. R. Doerr, M. Duelk and C. Dorrer, "107-gb/s optical signal generation using electronic time-division multiplexing," in *Journal of Lightwave Technology*, vol. 24, no. 8, pp. 3107-3113, 2006.
20. S. Khaleghi, O. F. Yilmaz, M. R. Chitgarha, M. Tur, N. Ahmed, S. R. Nuccio, I. M. Fazal, X. Wu, M. W. Haney, C. Langrock, M. M. Fejer and A. E. Willner, "High-Speed Correlation and Equalization Using a Continuously Tunable All-Optical Tapped Delay Line," in *IEEE Photonics Journal*, vol. 4, no. 4, pp. 1220-1235, 2012.
21. Y. Cao, M. Ziyadi, A. Mohajerin-Ariaei, A. Almaiman, P. Liao, C. Bao, B. Shamee, J. Yang, Y. Akasaka, M. Sekiya, M. Tur, C. Langrock, M. Fejer, J. Touch and A. Willner, "Reconfigurable optical inter-channel interference compensation of 20/25-Gbaud QPSK signals using nonlinear wave mixing," *Optical Communication (ECOC)*, 2015 European Conference on, paper P.3.17, Valencia, 2015, pp. 1-3.
22. S. Yamamoto, K. Saito, F. Hamaoka, T. Matsuda, A. Naka and H. Maeda, "Characteristics Investigation of High-Speed Multi-Carrier Transmission Using MIMO-Based Crosstalk Compensation in Homodyne Detection Scheme," in *Journal of Lightwave Technology*, vol. 34, no. 11, pp. 2824-2832, Jun. 1, 2016.
23. J. Treichler and M. Larimore, "New processing techniques based on the constant modulus adaptive algorithm," in *IEEE Transactions on Acoustics, Speech, and Signal Processing*, vol. 33, no. 2, pp. 420-431, Apr 1985.
24. D. Moss, R. Morandotti, A. Gaeta, and M. Lipson, "New CMOS-compatible platforms based on silicon nitride and Hydex for nonlinear optics," *Nature Photonics*, vol. 7, pp. 597–607, Jul. 30, 2013.